most remarkable improvement in the global CFR, as evidenced by a higher ratio of post- to pre-treatment CFR. Notably, that beneficial change was mainly caused by significant improvement in the basal left ventricle (control 0.9 ± 0.1 versus combined 1.4 ± 0.4 versus sheet-only 1.0 ± 0.1 versus OM-only 1.1 ± 0.1, respectively, ANOVA $P = 0.012$) (Figure 6e,f).

Global LV function and hemodynamic performance

The cardiac function was evaluated by echocardiography before (at baseline) and 2 and 4 weeks after each treatment ($n = 11$ for each group) (Figure 6 g,h). Two weeks after left coronary artery ligation, severe dilatation of the LV chamber and severe systolic dysfunction were observed, with no significant differences among the groups (Figure 6g). In the control, LV dimensions increased and LV ejection fraction deteriorated in a time-dependent manner, suggesting progressive LV remodeling. In the sheet-only and OM-only groups, LV ejection fraction initially improved, then tended to deteriorate in association with gradual LV dilatation. In the combined group, remarkable improvements in LV function parameters occurred promptly and were sustained for up to 4 weeks, resulting in significantly smaller LV dimensions and greater LV ejection fraction as compared with other treatment groups.

Consistently, the basic hemodynamic indices revealed that LV end-systolic pressure was higher, whereas LV end-diastolic pressure and time constant were lower in the combined group as compared to the others. Load-independent parameters assessed by pressure–volume loop analysis revealed that end-systolic pressure–volume relationship was higher, while end-diastolic pressure–volume relationship was lower in the combined group (Figure 6h). These results confirmed that cell-sheet therapy combined with OM-flap improved the therapeutic effects of single treatment group (cell-sheet only or OM-flap only) for the treatment of chronic MI.

Functional capacity assessment

There was no difference in running distance at 4 rpm (control 125 ± 15 versus combined 148 ± 9 versus sheet-only 133 ± 10 versus OM-only 135 ± 15 m, ANOVA $P = 0.63$) ($n = 11$ in each). In contrast, the combined group showed more improved functional capacity in terms of longer running distance at 8 rpm (54 ± 5 versus 178 ± 17 versus 81 ± 10 versus 76 ± 7 m, respectively, ANOVA $P < 0.001$).

Angiographic assessment of communication between coronary arteries and pedicle omentum

Communication between the coronary arteries and branches of the gastroepiploic artery in the OM specimens was evaluated using three different methods with a different series of OM-only and combined group animals ($n = 12$ in each) (Figure 1a).

A postmortem angiography examination from the aortic root was performed to verify antegrade flow from the OM into the heart in the combined and OM-only groups ($n = 4$ for each group). In the combined group, aortography revealed that the gastroepiploic artery branches feeding the OM expanded into the heart, and established several tight junctions between the native coronary arteries and OM (Figure 7a). In contrast, in the OM-only group, the gastroepiploic artery branches failed to penetrate the heart, accompanied by immature leaky collateral vessel formation between the coronary artery and OM, evidenced by considerable leakage of contrast agent (Figure 7b).

We selectively injected India ink into the celiac artery to visually and histologically confirm vessel communication between the pedicle OM and native coronary artery ($n = 4$ for each group). Numerous collaterals filled with India ink were clearly identified between the gastroepiploic artery and native coronary arteries in the combined group, while that was not seen in the OM-only group (data not shown) (Figure 7c–e). Histological analysis confirmed vessel communication between those in the combined group (Figure 7f,g).

Finally, a selective perfusion via aortic root and celiac artery using two different MICROFIL colors was performed ($n = 4$ for each group). In the combined group, MICROFIL solution injected in a retrograde manner into the aortic root (MV-117 Orange) was easily shown expanded into the OM to communicate with the gastroepiploic artery (Figure 7h). That solution injected into the celiac artery (MV-120 Blue) was also found to expand into the myocardium and communicated with native coronary arteries (Figure 7i). Those findings were not seen in the OM-only group (data not shown).

Vessel migration into cell-sheet from host myocardium and omentum

To further confirm whether the OM- and host myocardium-derived endothelial cells migrated toward the cell-sheet, we established two types of parabiotic pair models ($n = 4$ for each).

In parabiotic pairs of wild-type MI rats that received transplantation of cell-sheets labeled with Cell Tracker TM Orange CMTMR followed by coverage with a GFP-transgenic rat oriented pedicle OM, a large number of OM-derived endothelial cells (isolectin/GFP double-positive cells) had migrated toward the cell-sheet (Figure 8a–d). Similarly, in another parabiotic pair of GFP-transgenic MI rats that received cell-sheet transplantation covered with a wild-type rat oriented pedicle OM, a large number of host myocardium-derived endothelial cells (isolectin/GFP double-positive cells) had migrated toward the cell-sheet (Figure 8e–h).

Cell-sheet stimulated vascular cell migration

We performed an *in vitro* migration assay using HUVECs to evaluate the effects of skeletal myoblast cell-sheet derived growth factors on vessel recruitment (Figure 8i). The number of migrating cells was significantly greater in the 100% conditioned medium group, followed by the 10% conditioned medium and control groups, suggesting that SM cell-sheet derived growth factors stimulate vascular cell migration in a concentration-dependent manner (Figure 8j,k).

DISCUSSION

The major findings of this study can be summarized as follows. As compared to the single treatment groups, the cell-sheet plus OM group showed (i) improved donor cell retention along with amplified angiogenesis in the cell-sheet through the follow-up (at least day 28), (ii) attenuated cardiac hypertrophy and

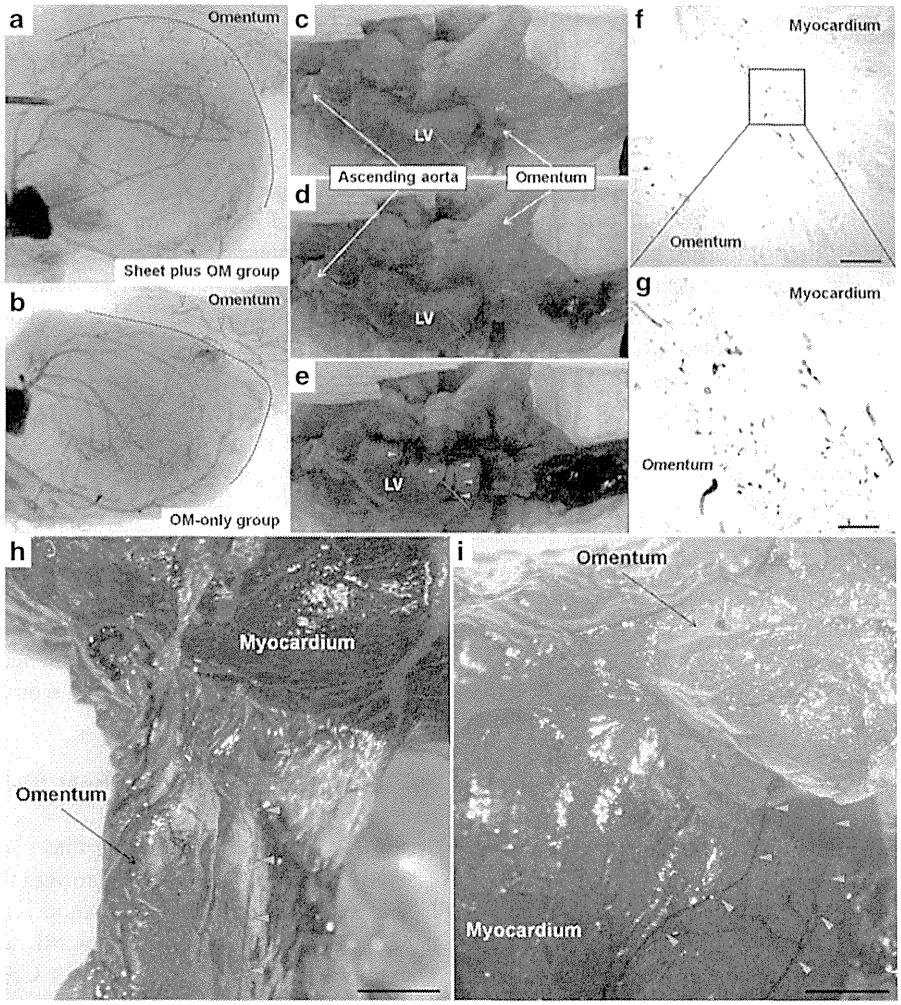

Figure 7 Communication between the coronary arteries and branches of the gastroepiploic artery was evaluated using three different methods with a different series of OM-only and combined group animals. A postmortem angiography examination from the aortic root in the combined (**a**) and OM-only (**b**) groups ($n = 4$ for each group). In the combined group, aortography revealed that the gastroepiploic artery branches feeding the OM expanded into the heart, and established several tight junctions between the native coronary arteries and OM (**a**). In contrast, in the OM-only group, the gastroepiploic artery branches failed to penetrate the heart, accompanied by immature leaky collateral vessel formation between the coronary artery and OM, evidenced by considerable leakage of contrast agent (red dotted circle) (**b**). Black dotted line indicates heart surface. Green triangles indicate the branches of the gastroepiploic artery. Selective India ink injection into the celiac artery to visually and histologically confirm vessel communication between the pedicle OM and native coronary artery ($n = 4$ for each group). Numerous collaterals filled with India ink were clearly identified between the gastroepiploic artery and native coronary arteries in the combined group (**c–e**), while that was not seen in the OM-only group (data not shown). Histological analysis confirmed vessel communication between those in the combined group (**f**: 40×, scale bar = 500 μm, **g**: 200×, scale bar = 100 μm). A selective perfusion via aortic root and celiac artery using two different MICROFIL colors ($n = 4$ for each group). In the combined group, MICROFIL solution injected in a retrograde manner into the aortic root (MV-117 Orange) was easily shown expanded into the OM to communicate with the gastroepiploic artery (**h**, 7.5×, scale bar = 2 mm). That solution injected into the celiac artery (MV-120 Blue) was also found to expand into the myocardium and communicated with native coronary arteries (**i**, 7.5×, scale bar = 2 mm). Those findings were not seen in the OM-only group (data not shown). Green triangles show visible vessel communication in the OM-flap (**h**) and host myocardium (**i**).

fibrosis, and a greater amount of functionally and structurally mature blood vessels in the ischemic myocardium, along with myocardial upregulation of relevant genes, (iii) increased vascularization in resistance arterial vessels with better dilatory responses to endothelium-dependent agents, (iv) more remarkable improvement in the global CFR, mainly caused by significant improvement in the basal left ventricle, (v) sustained improvements in cardiac function parameters and better functional capacity, and (vi) creation of robust vascular communication between the OM and native coronary arteries, shown by *in vivo* angiography.

The retention, survival, and engraftment of transplanted cells in the cell-sheet therapy are largely influenced by the degree of vascularization in the transplanted area and subsequent myocardial inflammation after cell-sheet transplantation.[2,17] The concept of combining OM-flap with the current cell-sheet therapy is likely to be reasonable because the OM is known to play a key role in controlling the spread of inflammation, and promoting revascularization, reconstruction and tissue regeneration. Our data suggest that the combined treatment improved the hypoxic environment in the transplanted area to a greater degree, potentially enhancing initial cell engraftment and enhancing the paracrine

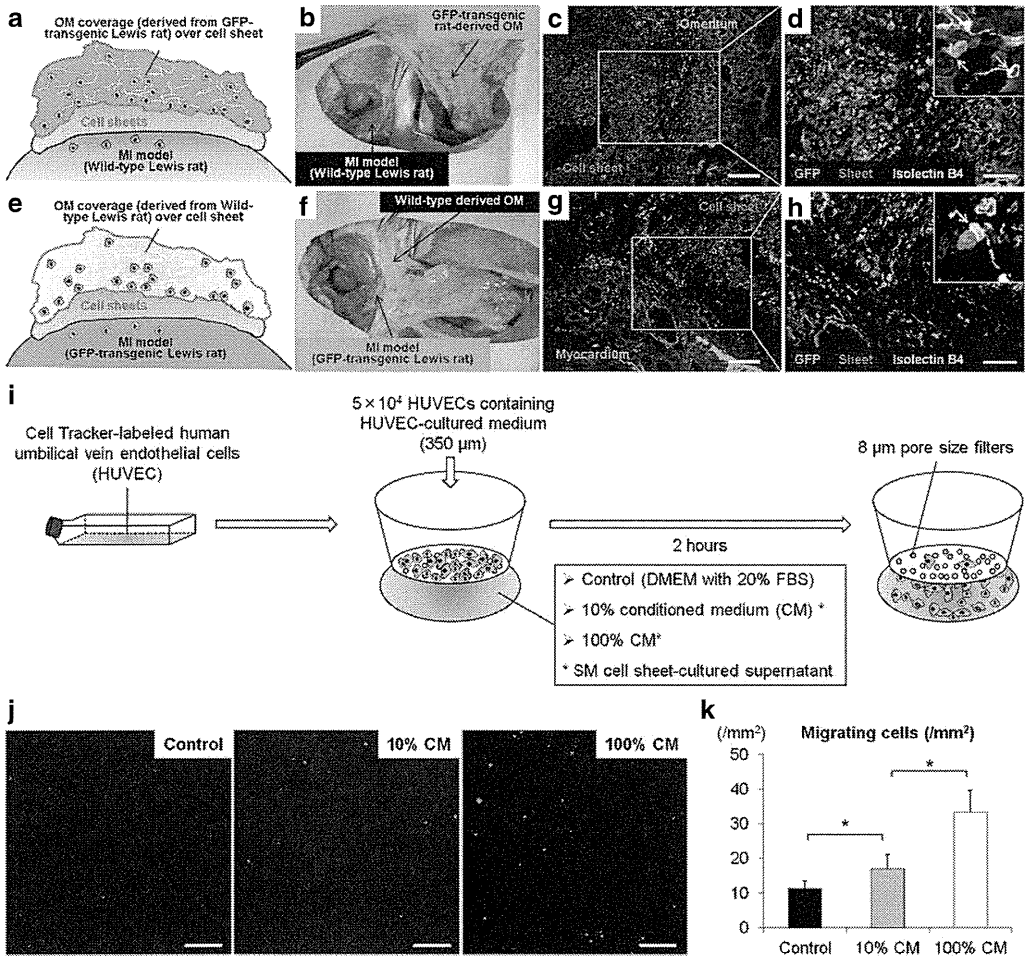

Figure 8 Schematic representation of experimental design to form parabiotic pairs of wild-type MI model rats (recipient) for transplantation of wild-type oriented cell-sheets labeled with Cell Tracker TM Orange CMTMR, followed by coverage with pedicle OM derived from GFP-transgenic rat (donor) (**a**,**b**). Representative GFP/isolectin staining in parabiotic pairs model (**c**: 100×, scale bar = 200 μm, **d**: 200×, scale bar = 100 μm). Schematic representation of experimental design to form second parabiotic pairs of GFP-transgenic MI rats for cell-sheet transplantation covered with wild-type oriented pedicle OM (**e**,**f**). Representative GFP/isolectin staining in second parabiotic pairs (**g**: 100×, scale bar = 200 μm, **h**: 200×, scale bar = 100 μm). *In vitro* migration assay (**i**). To investigate cell migration in response to skeletal myoblast cells cultured in conditioned medium, a modified Boyden chamber migration assay was performed using an HTS FluoroBlok Multiwell Insert System containing filters with a pore size of 8 μm. Human umbilical vein endothelial cells (HUVECs) were grown in EGM-2 culture medium. After incubation at 37 °C for 2 hours, the number of migrated cells was counted in 15 randomly chosen fields under 100× magnification using fluorescence microscopy. Two replicate samples were used in each experiment, which were performed at least twice. Migrating cells were analyzed using a light microscope and reported as numbers of migrating cells per mm² (**j**). Representative images show migrating cells labeled with Cell Tracker TM Orange CMTMR (100×, scale bar = 200 μm). Quantitative analyses of migrating cells according to concentration in the skeletal myoblast-cultured conditioned medium (**k**). Asterisk indicates statistical significance ($P < 0.05$).

effects induced by cell-sheet therapy in terms of higher expressions of relevant genes, potentially stabilizing therapeutic effect of cell-sheet therapy. The discrepancy between functional improvement and donor cell engraftment suggests that the improvement of cardiac function is not mainly mediated by direct contribution of transplanted donor cells but other indirect roles, possibly paracrine effects, offered by the cell-sheet at the early stage of transplantation.

The histological findings demonstrated that the rats receiving the cell-sheet implantation plus OM-flap had a significantly thickened anterior LV wall that was augmented by cardiomyocyte layers as compare to the other groups. Potential mechanisms may include cardiomyogenic differentiation of the donor-derived cells or endogenous stem cells, or paracrinal inhibition of progressive necrosis and/or apoptosis of the native cardiomyocytes. We speculate that both mechanisms might have contributed to the thickening of the targeted LV wall, although cardiomyogenic differentiation was not clearly identified in this study. Improved regional blood flow by the combined therapy could reduce the number of the necrotic/apoptotic cardiomyocytes, while reduced accumulation of fibrous components would inhibit thinning of the LV wall.[5,18] In addition, girdling effects from the covered OM might have reduced wall stress of the LV, leading to maintenance of the LV thickness.[19] Further studies to focus on the cardiomyogenic transdifferentiation using genetically labeled rodent models are warranted.

When blood vessels grow, endothelial cells migrate out first and assemble in a primitive network of immature channels

(angiogenesis).[5] As these nascent vessels only consist of endothelial cells, they rupture easily and are leaky, prone to regression, and poorly perfused.[18,20–22] Recruitment of mural cells around nascent vessels essentially contributes to remodeling and maturation of the primitive vascular network (arteriogenesis), subsequently causing therapeutic improvement of blood perfusion.[5,18] We found a larger percentage of vessels without lectin staining and lower maturation index in the control and single treatment groups, indicating that promotion of angiogenesis, but failure to effectively induce arteriogenesis. Consequently, the single treatments showed only transient effects on global cardiac function and limited functional capacity, possibly due to irregular capillary networks and increased vascular permeability. In the combined treatment group, greater numbers of functionally and structurally mature vessels were established promptly after treatment and maintained in ischemic myocardium. This might be primarily attributed to upregulated expressions of genes related to angiogenesis (*VEGF, VEGFR-1, VEGF-R2, Akt-1*) and/or endogenous regeneration (*SDF-1*). Moreover, elevated expressions of *Ang-1* and its receptor *Tie-2*, and *PDGF, VE-cadherin*, and *PECAM* might play key roles in promoting maturation processes such as "stabilization" of cell junctions and tight pericyte recruitment (arteriogenesis).[5,15,16,18,20–22] Interestingly, the elevated expression of the those relevant genes shown in the combined group was mostly reduced after 28 days after treatment (data not shown), corresponding with reduced donor cell presence. We found, however, the combined treatment group showed more sustained positive effects on vessel maturity and cardiac function recovery as compared with the control and single treatment groups at 28 days after treatment, indicating that paracrine mediators contribute to the myocardial recovery mainly during the early phase after the treatment and the effects on cardiac function and vessel structure, once established, could last for a longer time.[2] These data suggest that OM-flap covering the cell-sheet played a key role in accomplishing the maturity of the new vessels in the targeted myocardial territory, leading to formation of more organized and durable vascular network, as compared to the control and the single treatment groups.

Endothelial vasodilator function of coronary microvessels (resistance arterial vessels) is an important determinant of myocardial perfusion in response to increased myocardial oxygen demand, playing a critical role in neovascular therapies.[6–8] Vasodilation in response to specific endothelium-dependent and endothelium-independent stimuli within the coronary circulations can be measured to assess endothelial function. To the best of our knowledge, this is the first to verify that cell-sheet treatment with and without OM-flap could improve endothelial vasodilator function of resistance arterial vessels in a rat MI model, utilizing *in vivo* synchrotron-based microangiography that has proved an effective method for clearly visualizing resistance arterioles and accurately identifying neurohumoral modulation of coronary blood flow within the microcirculation for assessing therapy efficacy.[7,23,24] Microangiography revealed attenuated dilatation and a strong trend toward increased incidence of paradoxical constrictions in the control, followed by the single treatment group, suggesting that the endothelial-dependent vasodilator function in resistance arterial vessels was progressively impaired in those groups.[25,26] In contrast, combined treatment effectively restored endothelial function in resistance arterial vessels, evidenced by better dilatory responses to acetylcholine, an endothelium-dependent vasodilator.[27] This corresponds with PET/CT findings demonstrating substantial improvement in CFR, which indicated the ability of the myocardium to increase blood flow in response to increasing myocardial oxygen demand. Adenosine causes vasodilation by stimulating receptors in the microcirculation, facilitating measurement of the endothelium-independent CFR in the microcirculation. Interestingly, a remarkable improvement in CFR was observed in basal, but not apical LV, indicating that the combined treatment might be capable of improving microvasculature functionality of hibernating myocardium, rather than scar cardiac tissue. These physiological benefits in the coronary microcirculation may activate collateral growth through increased flow and shear stress, a powerful driving force of arteriogenesis, leading to enhanced functional capacity under a high load.[28,29] Therefore, we speculate that the present combined treatment strategy has potential to effectively prevent progression of endothelial dysfunction, which independently predicts major clinical adverse events in patients with heart failure.[28–30]

Our data suggest that the combination of cell sheet transplantation and OM-flap acts synergistically, rather than additively, on vessel maturation, coronary microcirculation physiology, functional capacity, and cardiac reverse remodeling, whereas the OM-only strategy failed to stabilize its long-term effect. These results encouraged us to investigate the role of the cell-sheet transplantation in activating the effects of OM-flap. Postmortem angiography findings demonstrated visible collateral vessels between the native coronary arteries and OM-flap in the combined group, whereas no tight junctions were shown in the OM-only group, indicating that formation of collateral vessels between native coronary arteries and OM was accelerated by the interposed cell-sheets. The possible mechanism of those findings might be explained by our *in vitro* migration assay demonstrating that growth factors and cytokines secreted by the cell-sheet stimulate migration of endothelial cells derived from both host myocardium and the OM toward the sheet, subsequently establishing robust vessel connections with persistent blood flow between the native coronary arteries and OM. In contrast, in the OM-only group, lack of that process caused immature leaky collateral vessel formation and thus inadequate collateral blood flow in the ischemic myocardium. Based on those findings, we speculate that the therapeutic effects of the combined treatment strategy might be responsible for increased donor cell survival and stimulation of donor cells induced by OM-flap as well as for cell-sheet–mediated activation of OM-flap as a donor artery with high perfusion capacity. Nevertheless, further studies are absolutely needed to determine the main molecular mechanism of therapeutic effects induced by the combined treatment.

LIMITATIONS

Considering the potential molecular mechanisms behind the beneficial histological and physiological alterations observed with the combined strategy, we found that a group of possibly relevant molecules including *VEGF-A*, *VEGF receptor-1*, *VEGF receptor-2*, *Akt-1*, *SDF-1*, *PDGF-β*, *Ang-1*, *Tie-2*, *VE-cadherin*, and *PECAM* were upregulated in the combined group, suggesting that the

effects may be attributed to activation of several paracrine molecules, rather than a single molecule. Although some may argue what kinds of cytokines play a major role in generating therapeutic effects among the many complex molecular and cellular mechanisms involved, we consider that establishment of mature vessels is a complex process that is not regulated by specific factors, but rather numerous multiple factors that also dynamically change in response to the process of angiogenesis or vessel maturation. We believe that use of a cell-sheet and pedicle-OM as synergistic intelligent engineered tissues can efficiently support the regenerative process by dynamic cross-talk with ischemic cardiac tissue.

Although we did not experience any complication such as torsion of omentum flap or diaphragmatic hernia in the rats receiving the combined treatment, it is considered that a conventional lapalotomy itself may adversely affect general conditions particularly in critically-ill heart failure patients. An endoscopic approach may be useful in minimizing the OM-flap procedure-related complications in clinical settings.

CONCLUSION

We demonstrated that cell-sheet transplantation with an omentum-flap better promoted arteriogenesis and improved coronary microcirculation physiology in ischemic myocardium tissue, leading to potent functional recovery in a rat MI model. Further development of this treatment strategy toward clinical application is encouraged.

MATERIALS AND METHODS

All experimental procedures were approved by an institutional ethics committee. Animal care was conducted humanely in compliance with the Principles of Laboratory Animal Care formulated by the National Society for Medical Research and the Guide for the Care and Use of Laboratory Animals, prepared by the Institute of Animal Resources and published by the National Institutes of Health (publication no. 85-23, revised 1996).

Two weeks after left coronary artery ligation, rats were divided into four groups: (i) skeletal myoblast cell-sheet transplantation covered with an OM-flap (combined group), (ii) cell-sheet transplantation only, (iii) OM-flap only, and (iv) sham operation (control group). The protocol of this study is shown in Figure 1a,b. All *in vivo* and *in vitro* assessments were carried out in a blinded manner. A detailed description of all methods and reagents used for the experiments is provided in the **Supplementary Materials and Methods**.

SUPPLEMENTARY MATERIAL

Figure S1. Frequency distribution charts showing individual segment caliber changes in response to acetylcholine in **(a)** third and **(b)** fourth branching order vessels.
Materials and Methods.

ACKNOWLEDGMENTS

We thank Tsuyoshi Ishikawa, Yuuka Fujiwara, Yuka Kataoka, Hiromi Nishinaka, Toshika Senba, and staff of the PET Molecular Imaging Center for their excellent technical assistance. This research was supported by Research on Regenerative Medicine for Clinical Application from the Ministry of Health, Labour and Welfare of Japan and the Australian Synchrotron International Synchrotron Access Program (ISAP AS-IA111). Experiments were performed at the Japan Synchrotron Radiation Research Institute (SPring-8, BL28B2, Proposal 2011A1169). T.S. is a consultant for CellSeed, Inc., and T.O. is an Advisory Board Member of CellSeed, Inc. and an inventor/developer holding a patent for temperature-responsive culture surfaces. The authors have no conflicts of interest to report.

REFERENCES

1. Shah, AM and Mann, DL (2011). In search of new therapeutic targets and strategies for heart failure: recent advances in basic science. *Lancet* **378**: 704–712.
2. Narita, T, Shintani, Y, Ikebe, C, Kaneko, M, Harada, N, Tshuma, N *et al.* (2013). The use of cell-sheet technique eliminates arrhythmogenicity of skeletal myoblast-based therapy to the heart with enhanced therapeutic effects. *Int J Cardiol* **168**: 261–269.
3. Sekiya, N, Matsumiya, G, Miyagawa, S, Saito, A, Shimizu, T, Okano, T *et al.* (2009). Layered implantation of myoblast sheets attenuates adverse cardiac remodeling of the infarcted heart. *J Thorac Cardiovasc Surg* **138**: 985–993.
4. Habib, GB, Heibig, J, Forman, SA, Brown, BG, Roberts, R, Terrin, ML *et al.* (1991). Influence of coronary collateral vessels on myocardial infarct size in humans. Results of phase I thrombolysis in myocardial infarction (TIMI) trial. The TIMI Investigators. *Circulation* **83**: 739–746.
5. Carmeliet, P and Jain, RK (2011). Molecular mechanisms and clinical applications of angiogenesis. *Nature* **473**: 298–307.
6. Gutiérrez, E, Flammer, AJ, Lerman, LO, Elízaga, J, Lerman, A and Fernández-Avilés, F (2013). Endothelial dysfunction over the course of coronary artery disease. *Eur Heart J* **34**: 3175–3181.
7. Shirai, M, Schwenke, DO, Tsuchimochi, H, Umetani, K, Yagi, N and Pearson, JT (2013). Synchrotron radiation imaging for advancing our understanding of cardiovascular function. *Circ Res* **112**: 209–221.
8. Furchgott, RF and Zawadzki, JV (1980). The obligatory role of endothelial cells in the relaxation of arterial smooth muscle by acetylcholine. *Nature* **288**: 373–376.
9. Banquet, S, Gomez, E, Nicol, L, Edwards-Lévy, F, Henry, JP, Cao, R *et al.* (2011). Arteriogenic therapy by intramyocardial sustained delivery of a novel growth factor combination prevents chronic heart failure. *Circulation* **124**: 1059–1069.
10. O'Shaugnessy, L (1937). Surgical treatment of cardiac ischemia. *Lancet* **232**: 185–194.
11. Takaba, K, Jiang, C, Nemoto, S, Saji, Y, Ikeda, T, Urayama, S *et al.* (2006). A combination of omental flap and growth factor therapy induces arteriogenesis and increases myocardial perfusion in chronic myocardial ischemia: evolving concept of biologic coronary artery bypass grafting. *J Thorac Cardiovasc Surg* **132**: 891–899.
12. Shrager, JB, Wain, JC, Wright, CD, Donahue, DM, Vlahakes, GJ, Moncure, AC *et al.* (2003). Omentum is highly effective in the management of complex cardiothoracic surgical problems. *J Thorac Cardiovasc Surg* **125**: 526–532.
13. Shudo, Y, Miyagawa, S, Fukushima, S, Saito, A, Shimizu, T, Okano, T *et al.* (2011). Novel regenerative therapy using cell-sheet covered with omentum flap delivers a huge number of cells in a porcine myocardial infarction model. *J Thorac Cardiovasc Surg* **142**: 1188–1196.
14. Kawamura, M, Miyagawa, S, Fukushima, S, Saito, A, Miki, K, Ito, E *et al.* (2013). Enhanced survival of transplanted human induced pluripotent stem cell-derived cardiomyocytes by the combination of cell sheets with the pedicled omental flap technique in a porcine heart. *Circulation* **128**(11 Suppl 1): S87–S94.
15. Mancuso, MR, Davis, R, Norberg, SM, O'Brien, S, Sennino, B, Nakahara, T *et al.* (2006). Rapid vascular regrowth in tumors after reversal of VEGF inhibition. *J Clin Invest* **116**: 2610–2621.
16. Inai, T, Mancuso, M, Hashizume, H, Baffert, F, Haskell, A, Baluk, P *et al.* (2004). Inhibition of vascular endothelial growth factor (VEGF) signaling in cancer causes loss of endothelial fenestrations, regression of tumor vessels, and appearance of basement membrane ghosts. *Am J Pathol* **165**: 35–52.
17. Shimizu, T, Sekine, H, Yang, J, Isoi, Y, Yamato, M, Kikuchi, A *et al.* (2006). Polysurgery of cell sheet grafts overcomes diffusion limits to produce thick, vascularized myocardial tissues. *FASEB J* **20**: 708–710.
18. Carmeliet, P and Conway, EM (2001). Growing better blood vessels. *Nat Biotechnol* **19**: 1019–1020.
19. Hagège, AA, Vilquin, JT, Bruneval, P and Menasché, P (2001). Regeneration of the myocardium: a new role in the treatment of ischemic heart disease? *Hypertension* **38**: 1413–1415.
20. Weis, SM and Cheresh, DA (2005). Pathophysiological consequences of VEGF-induced vascular permeability. *Nature* **437**: 497–504.
21. Cao, Y, Hong, A, Schulten, H and Post, MJ (2005). Update on therapeutic neovascularization. *Cardiovasc Res* **65**: 639–648.
22. Adams, RH and Alitalo, K (2007). Molecular regulation of angiogenesis and lymphangiogenesis. *Nat Rev Mol Cell Biol* **8**: 464–478.
23. Jenkins, MJ, Edgley, AJ, Sonobe, T, Umetani, K, Schwenke, DO, Fujii, Y *et al.* (2012). Dynamic synchrotron imaging of diabetic rat coronary microcirculation in vivo. *Arterioscler Thromb Vasc Biol* **32**: 370–377.
24. Iwasaki, H, Fukushima, K, Kawamoto, A, Umetani, K, Oyamada, A, Hayashi, S *et al.* (2007). Synchrotron radiation coronary microangiography for morphometric and physiological evaluation of myocardial neovascularization induced by endothelial progenitor cell transplantation. *Arterioscler Thromb Vasc Biol* **27**: 1326–1333.
25. Ludmer, PL, Selwyn, AP, Shook, TL, Wayne, RR, Mudge, GH, Alexander, RW *et al.* (1986). Paradoxical vasoconstriction induced by acetylcholine in atherosclerotic coronary arteries. *N Engl J Med* **315**: 1046–1051.
26. Marti, CN, Gheorghiade, M, Kalogeropoulos, AP, Georgiopoulou, VV, Quyyumi, AA and Butler, J (2012). Endothelial dysfunction, arterial stiffness, and heart failure. *J Am Coll Cardiol* **60**: 1455–1469.
27. Bonetti, PO, Lerman, LO and Lerman, A (2003). Endothelial dysfunction: a marker of atherosclerotic risk. *Arterioscler Thromb Vasc Biol* **23**: 168–175.
28. Poelzl, G, Frick, M, Huegel, H, Lackner, B, Alber, HF, Mair, J *et al.* (2005). Chronic heart failure is associated with vascular remodeling of the brachial artery. *Eur J Heart Fail* **7**: 43–48.
29. Meyer, B, Mörtl, D, Strecker, K, Hülsmann, M, Kulemann, V, Neunteufl, T *et al.* (2005). Flow-mediated vasodilation predicts outcome in patients with chronic heart failure: comparison with B-type natriuretic peptide. *J Am Coll Cardiol* **46**: 1011–1018.
30. Heitzer, T, Baldus, S, von Kodolitsch, Y, Rudolph, V and Meinertz, T (2005). Systemic endothelial dysfunction as an early predictor of adverse outcome in heart failure. *Arterioscler Thromb Vasc Biol* **25**: 1174–1179.

Figure S1

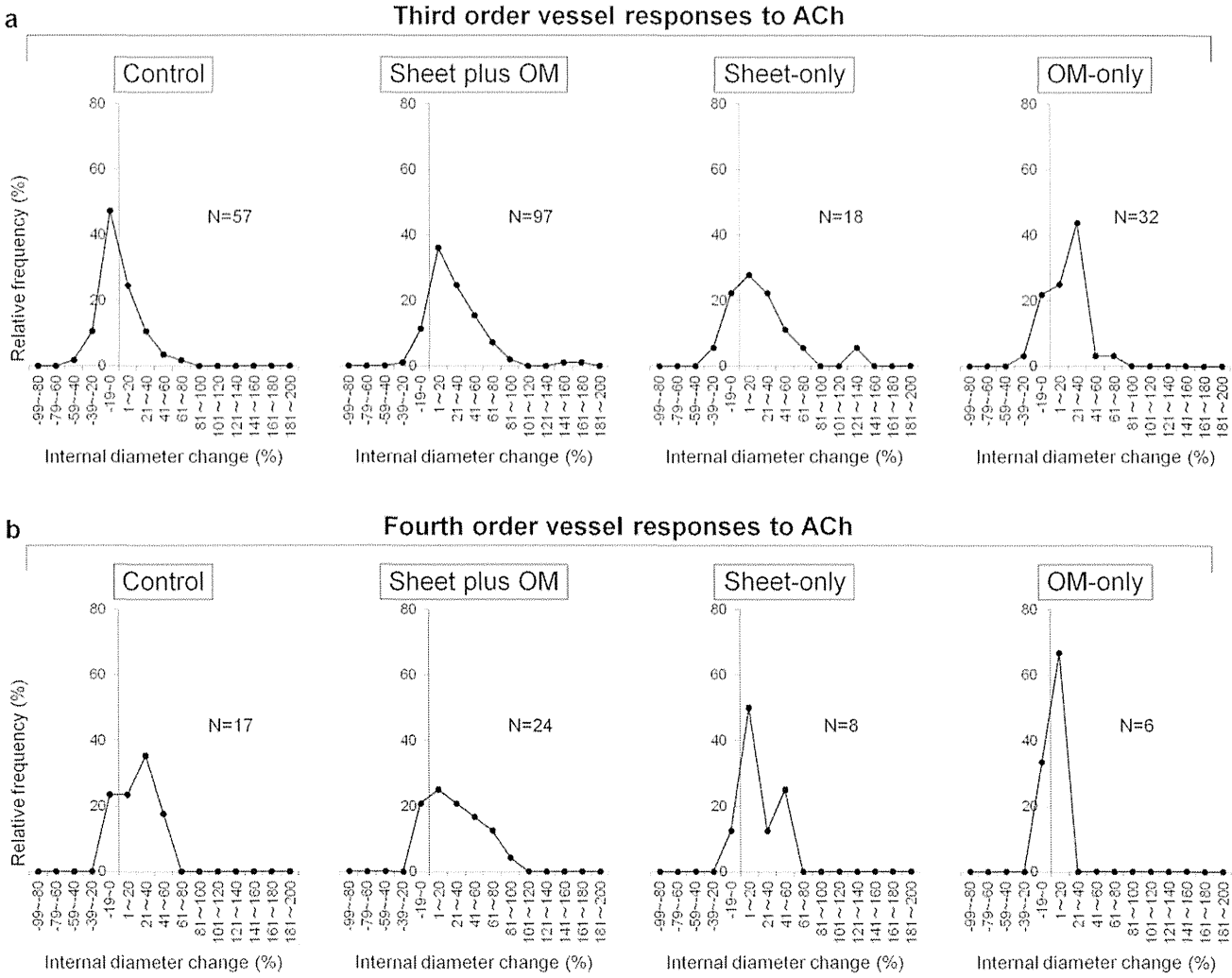
a
Third order vessel responses to ACh
Control
Sheet plus OM
Sheet-only
OM-only
N=57
N=97
N=18
N=32
Relative frequency (%)
Internal diameter change (%)
b
Fourth order vessel responses to ACh
Control
Sheet plus OM
Sheet-only
OM-only
N=17
N=24
N=8
N=6
Relative frequency (%)
Internal diameter change (%)

Supplemental figure legends

Figure S1

Frequency distribution charts showing individual segment caliber changes in response to acetylcholine in **(a)** third and **(b)** fourth branching order vessels. The control group had a relatively high frequency of third and fourth branching order arterial vessels showing localized segmental vasoconstriction (ID constriction >5% of baseline). The frequency of abnormal vasoconstriction with acetylcholine in the control group was about 8- and 4-fold for the third and fourth branching order, respectively, as compared with the combined group (third order: control 49% vs. combined 6% vs. sheet-only 22% vs. OM-only 25%; fourth order: control 18% vs. combined 4% vs. sheet-only 13% vs. OM-only 17%).

Supplemental Materials and Methods

Construction of Cell-sheets

Skeletal myoblasts were isolated from tibialis anterior muscle tissues of 3-week-old male wild-type or GFP transgenic Lewis rats as appropriate, and cultured as previously described.[1] In brief, when the cells became approximately 70% confluent after 4 days of cultivation in Dulbecco's modified Eagle Medium (DMEM) (Gibco) with 20% fetal bovine serum (Sigma-Aldrich), they were transferred to 35-mm temperature-responsive culture dishes (UpCell, Cellseed, Tokyo, Japan) and incubated at 37°C, with the cell number adjusted to 3.0×10^6 per dish. After 24 hours, the cells were induced to spontaneously detach by cooling at 20°C for 30 minutes, which yielded a scaffold-free sheet-shaped monolayer of skeletal myoblasts for use as a graft.

Establishment of Chronic Myocardial Infarction Rat Model

Two hundred female Lewis rats (180-200 g, Charles River) underwent left coronary artery ligation as previously described.[1] The rats were anaesthetized by inhalation of isoflurane (2%, 0.2 mL/min), intubated, and placed on a respirator during surgery to maintain ventilation. The carrier gas for isoflurane is oxygen. The adequacy of anaesthesia was monitored by electrocardiography and pulse rate. Two weeks after left coronary artery ligation, transthoracic echocardiography was performed to validate the extent of myocardial infarction (MI). We aimed to create a widespread MI model, thus rats with a small extent of wall motion abnormality with ejection fraction greater than 45% were excluded **(Figure 1)**. The widespread chronic MI models were randomly divided into 4 treatment groups: 1) cell-sheet transplantation covered with omentum (OM)-flap (combined group), 2) cell-sheet transplantation (sheet-only group), 3) OM-flap (OM-only group), and 4) sham operation

(control group) **(Figure 1)**. In the sheet-only group, a five-layered cell-sheet was placed on the area and spread manually to cover both infarct and border areas. In the OM-only group, a small upper midline laparotomy was performed to manipulate the OM tissue. After making a small hole in the diaphragm, the pedicle OM-flap was then pulled from the peritoneal space to the pleural cavity using a transdiaphragmatic approach and wrapped directly onto the epicardium in the ischemic area. In the combined group, 5-layered cell-sheets were placed in a similar manner as in the sheet-only group, then covered with the harvested OM-flap.

Histological Analysis

Four weeks after the treatment, the rats were humanely killed by an intraperitoneal injection of pentobarbital (300 mg/kg) and heparin (150 U) for histological analysis of the heart tissue (n=11 for each group) **(Figure 1)**. Anterior wall thickness was measured in at least 3 hematoxylin and eosin-stained sections of the middle portion of the LV, while Sirius red staining was performed to assess myocardial fibrosis in the peri-infarct region. The fibrotic region was calculated as the percentage of myocardial area. Data were obtained from 5 individual views of each heart. Periodic acid-Schiff staining was performed to examine the degree of cardiomyocyte hypertrophy. Myocyte size was determined by drawing point-to-point perpendicular lines across the cross-sectional area of the cell at the level of the nucleus. The results are expressed as the average diameter of 20 myocytes randomly selected from 5 fields of each ventricle. The images were examined by optical microscopy (Olympus, Tokyo, Japan) and quantitative morphometric analysis for each sample was performed using Metamorph software (Molecular Devices, Sunnyvale, California, US).

RNA Extraction and Quantitative Reverse-transcription Polymerase Chain Reaction

The myocardial gene expressions related to angiogenesis, vessel maturation, and anti-inflammation at 3 days after the treatment were assessed by quantitative reverse transcription PCR **(Figure 2)**. Total RNA was extracted from the peri-infarct myocardium using an RNeasy mini kit (Qiagen GmbH, Hilden, Germany), according to the manufacturer's instructions. For each sample, 1 μg of total RNA was converted to cDNA with Omniscript RT (Qiagen) and analyzed with a PCR array (Qiagen-SABiosciences) and Applied Biosystems® ViiA™ 7 real-time PCR system (Life Technologies Corporation). Data were normalized to β-actin expression level. Relative gene expression was determined using the ΔΔCT method.

Immunohistochemistry

Endothelial cells were labeled with rat monoclonal anti-CD31 antibody (Abcam, Cambridge, UK 1:50), while pericytes were labeled with mouse monoclonal anti-α-SMA antibody (DAKO, Glostrup, Danmark 1:50) and visualized by corresponding secondary antibodies (Alexafluor 488 or Alexafluor555; Alexafluor 647 Molecular Probes, Eugene, OR), then counterstained with Hoechst 33342 (Dojindo, Kumamoto, Japan). Vessel density and maturity were quantified as the number of CD31 positive vessels and CD31/α-SMA double-positive vessels per mm^2, respectively. A maturation index was calculated as the percentage of CD31/α-SMA double-positive vessels to total vessel number. Vessels positive for CD31 but negative for lectin were regarded as functionally immature vessels undergoing regression or that had lost patency.[2]

Evaluation of Mature Vessels with Patent Endothelial Layers

Mature vessels with patent endothelial layers were assessed by injection of 500 μl of Alexa Fluor 568 conjugate-labeled esculentum lectin (500 μg in 500 uL in 0.9% NaCl; GS-IB4,

Molecular Probes, Eugene, OR), which binds uniformly and rapidly to the luminal surface of endothelium and thus labels patent blood vessels, into a tail vein 30 minutes before tissue sampling.[2] Myocardial tissues were then removed, immersed in fixative for 1 hour in 4% paraformaldehyde, rinsed several times with PBS, infiltrated with 30% sucrose, frozen in OCT compound, and processed for immunohistochemistry.

Vessel Recruitment in the Transplanted Cell-sheets

To evaluate the angiogenic effect of the OM-flap in the transplanted area, we serially assessed the number of functional blood vessels with patent endothelial layers (CD31/lectin double-positive cells) in the transplanted area of the sheet-only and combined groups at 3, 7 and 28 days after each treatment (n=6 for each group and each time point) **(Figure 3)**.

Vessel Remodeling and Maturation in Peri-infarct Myocardium

We serially assessed neovascular vessel maturity in peri-infarct areas at 3 (n=6 for each group) and 28 days (n=11 for each group) after treatment **(Figure 4)**. Vessel density and structural maturity were quantified as the number of CD31 positive and CD31/α-smooth muscle actin (SMA) double-positive vessels per mm^2, respectively. A maturation index was calculated as the percentage of CD31/α-SMA double-positive vessels to total vessel number.

Synchrotron radiation microangiography

To evaluate the effects of each treatment on microcirculation physiology in terms of relative dilatory responses to acetylcholine and dobutamine hydrochloride in the resistance vessels, synchrotron radiation microangiography was performed after 3 weeks after the treatment (control: n=11, combined: n=11, cell-sheet: n=5, OM: n=6) at SPring-8, Japan Synchrotron

Radiation Research Institute, Hyogo, Japan with approval from the Animal Experiment Review Committee in accordance with the guidelines of the Physiological Society of Japan, as previously described **(Figure 4)**.[3] In brief, under sodium pentobarbital anesthesia (50 mg/kg i.p.), examined rats were intubated and artificially ventilated (Shinano, Tokyo, Japan; 40% oxygen), then the right carotid artery was cannulated with a radiopaque 20-gauge BD Angiocath catheter (Becton Dickinson, Inc., Sandy, Utah, USA), placing the tip at the entrance of the aortic valve. Each rat was then placed in line with the horizontal X-ray beam and SATICON detector system (Hitachi Denshi Techno-system, Ltd., Tokyo, Japan and Hamamatsu Photonics, Shizuoka, Japan). Iodinated contrast medium (Iomeron 350; Bracco-Eisai Co. Ltd, Tokyo, Japan) was injected intrarterially as a bolus (0.3-0.5 ml at 0.4 ml/s) into the aorta using a clinical autoinjector (Nemoto Kyorindo, Tokyo, Japan) at the start of image recording scanning. At least 10 minutes was allowed for renal clearance of the contrast between imaging scans. Following a baseline recording, an endothelium-dependent vasodilatory response was recorded as an angiogram series at the end of a 5-minute infusion of acetylcholine (5 μg/kg/min). A third image series was recorded after a 5-minute infusion of dobutamine hydrochloride (8 μg/kg/min) to assess the ability to maintain perfusion of the infarcted region during increased heart work.

Assessment of Vessel ID during Synchrotron Angiography

Quantitative analysis of vessel internal diameter (ID) was based on measurements from the middle of discrete vessel segments in individual cine-radiogram frames using Image-J (v1.41, NIH, Bethesda, USA) for individual rats during each treatment period. Arterial vessels were categorized according to their branching order.[3] The results for vessel ID in each rat during drug infusions are expressed as percentage changes from baseline (Δ), to account for

differences in absolute baseline vessel ID among the groups.

Quantification of Segmental Vasoconstrictions during Synchrotron Angiography

The relative change in vessel caliber in response to vasoactive agents gives no indication of vessel number with calibers less than the individual's mean change. Therefore, the number of abnormal vasoconstrictions during treatment periods was quantified. Localized segmental vasoconstrictions were considered to be present when a vessel segment showed an ID constriction of >5% of baseline vessel ID value.[3,4]

PET measurements and data analysis

To evaluate the effects of each treatment on global and regional myocardial blood flow (MBF) and coronary flow reserve (CFR), ^{13}N-ammonia PET measurements were serially performed 1 day before and 3 weeks after treatment (control: n=5, combined: n=8, cell-sheet: n=7, OM: n=7) **(Figure 5)**. Rats were anesthetized with 2% isoflurane plus 100% oxygen and a cannula was inserted into the tail vein. PET data were acquired using a small animal PET device (Inveon PET/CT system, Siemens). Dynamic 10-minute PET measurements were started with an administration of ^{13}N-NH_3 over 20 seconds (approximately 20 and 80 MBq for the rest and stress study, respectively).[5] The stress study was performed 5 minutes after bolus injection of CGS-21680 (5 μg/kg), a selective adenosine A2A agonist that induced coronary vasodilatation and increases in the MBF.

The PET data were reconstructed into 23 frames (12 fr × 5 s, 6 fr × 10 s, 4 fr × 30 s, 1 fr × 360 s) using the 3-dimensional ordered subset expectation maximization method followed by maximum a posteriori (3D-OSEM/MAP). Regions of interest were semi-automatically placed on the left ventricle myocardium and blood pooled inside the left and right ventricle, with

reference to the summed PET and CT images. MBF was calculated using the one-tissue compartment model developed by DeGrado et al. with PMOD software.[6] Global and regional MBF (basal, mid, apical segments) were used for the evaluations.[7] CFR was expressed as the ratio of MBF during stress to MBF at rest. Change in CFR was evaluated as the ratio of post-treatment to pre-treatment CFR. Normal male SD rats (n=6, 10-11 weeks old, BW: 369-429 g) were used for the validation study for quantitative PET measurements with a stress agent.

Assessment of Cardiac Function

The cardiac function was evaluated by echocardiography 2 and 4 weeks after each treatment (n=11 for each group) **(Figure 6)**. Baseline measurements were made before each treatment. Transthoracic echocardiography was performed with using a SONOS 5500 (Philips Electronics, Tokyo, Japan) equipped with a 12-MHz annular array transducer under general anaesthesia induced and maintained by inhalation of isoflurane (2%, 0.2 mL/min) as mentioned above **(Figure 1)**. The hearts were imaged in short-axis 2D views at the level of the papillary muscles, and the LV end-systolic and end-diastolic dimensions were determined. LV ejection fraction was calculated by Pombo's method.

LV pressure-volume loop analysis with cardiac catheterization was performed for each group as previously described.[1] In brief, a median sternotomy was performed and the LV apex was carefully dissected to minimize hemorrhaging. A MicroTip catheter transducer (SPR-671; Millar Instruments, Inc, Houston, Tex) and conductance catheter (Unique Medical Co, Tokyo, Japan) were then placed longitudinally into the left ventricle from the apex. LV pressure-volume relationships were determined by transiently compressing the inferior vena cava.

Exercise Tolerance

Eleven rats in each group were acclimated to a rodent activity wheel (MULTI-FUNCTIONAL ACTIVITY WHEEL, MK-770M, Muromachi, Tokyo, Japan) by running daily for 5 days. During the acclimation period, the round speed was increased from 5 to 10 rpm, with the exercise duration maintained at 20 minutes. On the day of tolerance testing, animals were placed on the activity wheel at round speeds of 4 or 8 rpm and allowed to exercise until fatigue. Fatigue was defined as the point at which the animal failed to keep pace with the activity wheel despite constant physical prodding for 1 minute. Running distance was used as an index of maximal capacity for exercise.

Communication Between Pedicle Omentum and Native Coronary Artery

Communication between the coronary arteries and branches of the gastroepiploic artery in the OM specimens was evaluated using 3 different methods in a different series of OM-only and combined group (n=12 for each group) **(Figure 7)**.

Aortic Root Angiography using Barium Sulfate

We performed a postmortem angiography examination from the aortic root to verify antegrade flow from the OM into the heart (n=4 for each). In brief, a catheter with an internal diameter of 0.89 mm (COVIDIEN Ltd, Tokyo, Japan) was inserted from the right carotid artery into the aortic root, followed by systemic heparinization (1000 IU heparin). The rats were euthanized with an overdose of pentobarbital, then an incision was made in the right jugular vein and lactated Ringer's solution was manually perfused through the cannula for 5 minutes. Approximately 3 mL of a solution consisting of 70% weight/volume barium sulfate

suspended in 7% gelatin was then injected in a retrograde manner via the catheter using a programmed syringe pump. Angiograms were obtained with a angiographic system (MFX-80HK, Hitex) consisting of an open type 1-μm microfocus X ray source (L9191, Hamamatsu Photonics) and a 50/100 mm (2"/4") dual mode X-ray image intensifier (E5877JCD1-2N, Toshiba) set at 60 kV and 60 μA.

Selective India Ink Perfusion via Celiac Artery

Next, we selectively injected India ink into the celiac artery to visually and histologically confirm vessel communication between the pedicle OM and native coronary artery (n=4 for each). The catheter was inserted via the abdominal aorta and its tip placed near the celiac artery, followed by systemic heparinization. The chest was reopened to expose the wrapped heart, taking care to avoid injuring the OM. The heart was harvested after perfusion fixation of the vasculature, as described above. We ligated the abdominal aorta just proximal from the tip of the catheter in advance and selectively injected India ink via the celiac artery into the heart, and then performed histological analysis.

Selective Perfusion via Aortic Root and Celiac Artery Using Two Different MICROFIL Colors

A catheter was inserted from the right carotid artery into the aortic root and another was inserted from the abdominal aorta into the celiac artery, followed by systemic heparinization (1000 IU heparin). After perfusion fixation, we ligated the abdominal aorta just proximal from the tip of the catheter. Approximately 3 mL of 2 different colors of MICROFIL solution (MICROFIL Silicone Rubber Injection Compounds, Flow Tech, Inc.) was injected in an antegrade manner into the celiac arterial trunk (MV-120 Blue) and a retrograde manner from

the aortic root into the coronary artery (MV-117 Orange). The solution was allowed to solidify for more than 30 minutes. The heart and OM were removed en bloc, and placed in 10% neutral buffered formalin for several days. The tissue was then cleared using sequential 24-hour incubations in 25% ethanol, 50% ethanol, 75% ethanol, 95% ethanol, 100% ethanol, and methylsalicylate, according to the manufacturer's instructions. Evidence of vessel communication between the native coronary artery and OM-flap was photographed in multiple planes using an Olympus DP70 camera attached to an Olympus SZX 12 stereo microscope (Olympus, Tokyo, Japan).

Creation of Surgically Joined Parabiotic Pairs Model

To further confirm whether the OM- and host myocardium-derived endothelial cells migrated toward the cell-sheet, we established two types of parabiotic pair models (n=4 for each) **(Figure 8)**. To determine whether OM-derived endothelial cells migrated toward the cell-sheet, the parabiotic pairs model were established by producing wild-type MI model rats (recipient) to receive transplantation of wild-type oriented cell-sheets which was labeled with Cell Tracker TM Orange CMTMR (Invitrogen, Oregon, USA), followed by coverage with a pedicle OM derived from a transgenic ubiquitously expressing GFP rat (donor) and then surgically joining them. Similarly, to determine whether host myocardium-derived endothelial cells migrated toward the cell-sheet, we also established another parabiotic pairs model by producing GFP-transgenic MI model rats (recipient) to receive transplantation of wild-type oriented cell-sheets which was labeled with Cell Tracker TM Orange CMTMR, followed by coverage with a pedicle OM derived from a wild-type rat (donor) and then surgically joining them.

Parabiotic pair rats were anaesthetized by inhalation of isoflurane (2%, 0.2 mL/min) and

maintained for 72 hours under mechanical ventilation with a continuous infusion of 5% glucose (0.3 ml/h), then subjected to histological analyses.

In vitro Migration assay

To investigate cell migration in response to skeletal myoblast cells cultured in conditioned medium, a modified Boyden chamber migration assay was performed using an HTS FluoroBlok™ Multiwell Insert System (BD Falcon, NJ, USA) containing filters with a pore size of 8 μm. Briefly, human umbilical vein endothelial cells (HUVECs) (purchased from Lonza) were grown in EGM-2 culture medium (Lonza, Walkersville, USA). To visualize them, HUVECs were stained in advance with Cell Tracker TM Orange CMTMR (Invitrogen, Oregon, USA). A suspension of 5×10^4 HUVECs in HUVEC-cultured medium (350 μm) was applied to each upper chamber. The lower chamber was filled with 1.0 ml of concentrated skeletal myoblasts-cultured supernatant composed of DMEM with 20% fetal bovine serum (100% conditioned medium), 10-fold diluted conditioned medium (10% conditioned medium) or DMEM, and 20% fetal bovine serum (control group). After incubation at 37°C for 2 hours, the number of migrated cells was counted in 15 randomly chosen fields under 100×magnification using fluorescence microscopy (BIOREVO BZ-9000, KEYENCE, Osaka, Japan). Two replicate samples were used in each experiment, which were performed at least twice. Migrating cells were analyzed using a light microscope and reported as numbers of migrating cells per mm^2.

Statistical analysis

Data are expressed as the mean ± SEM unless otherwise stated. Student's t test (2 tailed) was used to compare 2 groups of independent samples. One-way and two-way ANOVA with

Bonferroni correction for repeated measures were performed to assess within and between group differences following the treatments. Following ANOVA, between group comparisons were made using a Student's t-test (2-tailed). Multiplicity in pairwise comparisons was corrected by the Bonferroni procedure. The Statistical Package Software System (SPSS v15, SPSS Inc, Chicago, USA) and JMP 9.0 (SAS Institute Inc, Cary, NC) were used for all analyses, with P values <0.05 deemed to indicate significance.

References

1. Sekiya N, Matsumiya G, Miyagawa S, Saito A, Shimizu T, Okano T, Kawaguchi N, Matsuura N, Sawa Y. Layered transplantation of myoblast sheets attenuates adverse cardiac remodeling of the infarcted heart. *J Thorac Cardiovasc Surg* 2009;**138**:985-993.
2. Mancuso MR, Davis R, Norberg SM, O'Brien S, Sennino B, Nakahara T, Yao VJ, Inai T, Brooks P, Freimark B, Shalinsky DR, Hu-Lowe DD, McDonald DM. Rapid vascular regrowth in tumors after reversal of VEGF inhibition. *J Clin Invest* 2006;**116**:2610-2621.
3. Jenkins MJ, Edgley AJ, Sonobe T, Umetani K, Schwenke DO, Fujii Y, Brown RD, Kelly DJ, Shirai M, Pearson JT. Dynamic synchrotron imaging of diabetic rat coronary microcirculation in vivo. *Arterioscler Thromb Vasc Biol* 2012;**32**:370-377.
4. Ludmer PL, Selwyn AP, Shook TL, Wayne RR, Mudge GH, Alexander RW, Ganz P. Paradoxical vasoconstriction induced by acetylcholine in atherosclerotic coronary arteries. *N Engl J Med* 1986;**315**:1046-1051
5. Croteau E, Bénard F, Bentourkia M, Rousseau J, Paquette M, Lecomte R. Quantitative myocardial perfusion and coronary reserve in rats with 13N-ammonia and small animal PET: impact of anesthesia and pharmacologic stress agents. *J Nucl Med* 2004;**45**:1924-1930.
6. DeGrado TR, Hanson MW, Turkington TG, Delong DM, Brezinski DA, Vallée JP, Hedlund LW, Zhang J, Cobb F, Sullivan MJ, Coleman RE. Estimation of myocardial blood flow for longitudinal studies with 13N-labeled ammonia and positron emission tomography. *Med J Nucl Cardiol* 1996;**3**:494-507.
7. Cerqueira MD, Weissman NJ, Dilsizian V, Jacobs AK, Kaul S, Laskey WK, Pennell DJ, Rumberger JA, Ryan T, Verani MS; American Heart Association Writing Group on Myocardial Segmentation and Registration for Cardiac Imaging. Standardized myocardial